JACS
JOURNAL OF THE AMERICAN CHEMICAL SOCIETY

Article

Construction of Acyclic Quaternary Carbon Stereocenters by Catalytic Asymmetric Hydroalkynylation of Unactivated Alkenes

Zi-Xuan Wang, and Bi-Jie Li

J. Am. Chem. Soc., **Just Accepted Manuscript** • Publication Date (Web): 22 May 2019

Just Accepted

is published by the American Chemical Society. 1155 Sixteenth Street N.W., Washington, DC 20036

Construction of Acyclic Quaternary Carbon Stereocenters by Catalytic Asymmetric Hydroalkynylation of Unactivated Alkenes

Zi-Xuan Wang and Bi-Jie Li*

Center of Basic Molecular Science (CBMS), Department of Chemistry, Tsinghua University, Beijing, 100084, China.

ABSTRACT: Quaternary carbon stereocenters are common structural motifs in organic synthesis. The construction of these stereocenters in a catalytic and enantioselective manner remains a prominent synthetic challenge. In particular, methods for the synthesis of alkyne-substituted quaternary carbon stereocenters are very rare. Previous catalytic systems for hydroalkynylation of alkenes create tertiary stereocenters. We describe here an iridium catalyzed asymmetric hydroalkynylation of non-activated trisubstituted alkene. The hydroalkynylation of β,γ-unsaturated amides occurs with high regio- and enantio-selectivities to afford alkyne-substituted acyclic quaternary carbon stereocenters. Computational and experimental data suggest that the enantioselectivity is not only determined by the facial selectivity of the alkene but also by an alkene isomerization process. This strategy provides an efficient method to access alkyne-substituted acyclic quaternary carbon stereocenters with minimally functionalized starting materials.

I. Introduction

Quaternary carbon stereocenters occur frequently in natural products, drugs and bioactive molecules.[1] For example, 12% of the top 200 prescription drugs sold in the US in 2011 contain quaternary carbon stereocenters.[2] However, all quaternary carbon stereocenters in these molecules are derived from natural product precursors rather than being built through chemical synthesis. These situation reflects the longstanding challenges associated with the construction of quaternary carbon stereocenters, especially in acyclic systems due to the enhanced conformational mobility.[3]

The alkynyl group is a common functionality in organic synthesis. It can be easily transformed to an alkenyl, alkyl, heteroaryl or carboxylic acid group.[4] Thus, construction of alkyne substituted quaternary carbon stereocenters, coupled with subsequent transformations of the alkyne group, would enable access to various functionalized quaternary stereocenters. However, transition metal-catalyzed enantioselective synthesis of alkyne-substituted quaternary carbon stereocenters is very limited (Scheme 1). For example, the groups of Nishibayashi,[5] Carreira,[6] and Song[7] have reported elegant propargylation methods to access quaternary carbon stereocenters, respectively. Czekelius and co-workers have developed enantioselective synthesis of alkyne substituted quaternary stereocenter through desymmetrization of diynamides.[8] We are aware of only one example that generates alkyne-substituted all-carbon quaternary stereocenter through metal-catalyzed alkynyl addition. The Hoveyda group has achieved Cu-catalyzed highly enantioselective allylic substitution with alkynyl aluminum reagents.[9] Despite these notable advances, methods for catalytic asymmetric synthesis of alkyne-substituted quaternary carbon stereocenters from minimally functionalized starting materials are highly desirable.[10]

Asymmetric hydroalkynylation of alkenes with terminal alkyne would be an ideal approach for the construction of alkyne-substituted quaternary carbon stereocenters because this process is atom-economical and make use of unfunctionalized materials.[11] However, we are mindful of several issues for this process to become successful. First, the catalyst must be capable of overcoming significant steric hindrance for the formation of quaternary carbon stereocenters. Current catalytic systems for hydroalkynylations are limited to di-substituted alkenes including α,β-unsaturated compounds[12] and activated alkenes,[13] leading to the formation of alkyne-substituted tertiary carbon stereocenters.[14] Second, the catalyst must exert substantial regio-control because the hydroalkynylation could occur at the less substituted site of the alkene. Third, the catalyst should suppress undesired alkene isomerization because it could lead to diminished regioselectivity and enantioselectivity. Consequently, highly enantioselective alkene hydroalkynylation that generate all-carbon quaternary stereocenters remains undeveloped.

Scheme 1. Metal-Catalyzed Construction of Alkyne-Substituted Quaternary Carbon Stereocenters

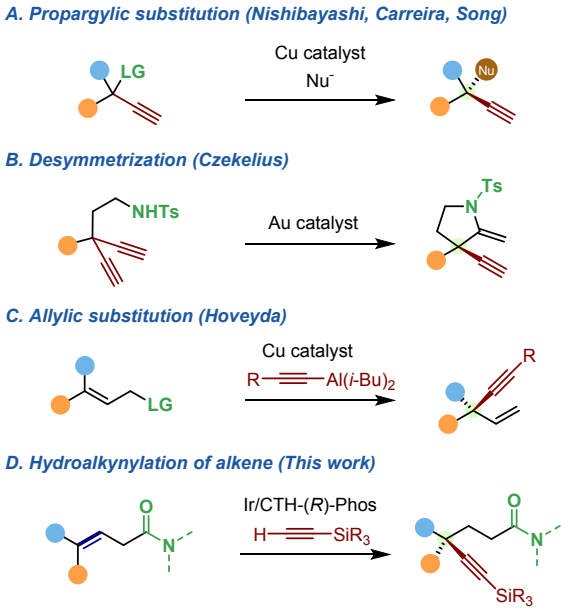

Herein, we report a highly regio- and enantioselective hydroalkynylation of nonactivated trisubstituted alkenes

assisted by an amide group.[15,16] The catalytic alkynylation occurs selectively at the more substituted site remote to the amide group, providing a method for the generation of stereocenter distal to a functional group.[3j,17] Combined experimental and computational studies suggest that the enantioselectivity is controlled by facial selection of the alkene and an alkene isomerization process. This strategy provided an unprecedented synthetic entry to construct alkyne-substituted acyclic quaternary carbon stereocenters.

II. Results and discussion

Table 1. **Reaction Development** [a]

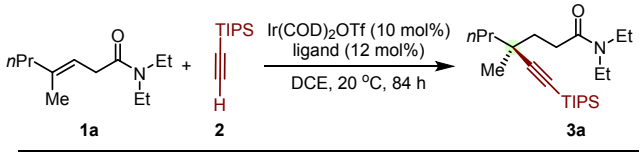

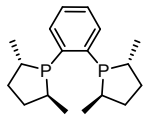

L1, (*S*,*S*)-Me-DuPhos
<5%

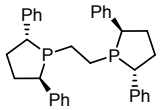

L2, (*S*,*S*)-Ph-BPE
<5%

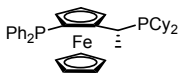

L3, (*R*, S_p)-Josiphos
<5%

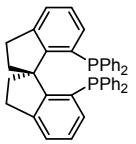

L4, (*R*)-SDP
<5%

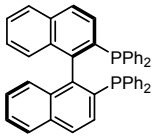

L5, (*R*)-BINAP
44%, 91:9 er

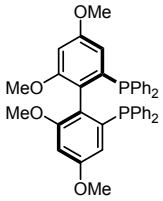

L6, (*R*)-GarPhos
37%, 90:10 er

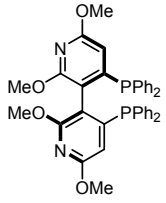

L7, CTH-(*R*)-P-Phos

DCE	62%, 94.5:5.5 er
THF	<5%, N. D.
$CHCl_3$	72%, 93.5:6.5 er
toluene	<5%, N. D.
C_6H_5F	33%, 94.5:5.5 er
o-$C_6H_4F_2$	65%, 95:5 er

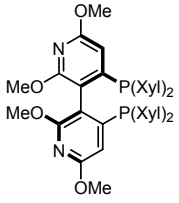

L8, CTH-(*R*)-Xyl-P-Phos
23%, 95:5 er

[a] Reaction conditions: **1a** (1.0 equiv.), **2** (2.0 equiv.), 20 °C, 84 h. Isolated yields were reported. The er values were determined by HPLC on a chiral stationary phase. N. D., not determined.

2.1 Reaction Development. We began by testing the combination of $Ir(COD)_2OTf$ and a series of chiral ligands to effect the hydroalkynylation of β,γ-unsaturated tertiary amide **1a** with triisopropylsilylacetylene **2** (Table 1). Me-Duphos (**L1**) and Ph-BPE (**L2**), which could promote the hydroalkynylation of enamides, did not show any activity in the current reaction. The use of bis(phosphine) ligands including Josiphos based on ferrocene (**L3**) and a spirocyclic ligand SDP (**L4**)[18] did not provide significant amount of alkynylation product either. When BINAP (**L5**) was used as a ligand, 44% yield of the alkynylation product with 91:9 enantiomeric ratio (er) was observed. Notably, the alkynylation occurs regioselectively at the γ position instead of the less hindered β position. This result led us to evaluate structurally related bis(phosphine) ligands. With Garphos (**L6**) as a ligand, we observed similar enantioselectivity compared to the result obtained with BINAP but in lower yield of the desired product. When the ligand was switched to CTH-P-Phos (**L7**), hydroalkynylation product **3a** was obtained in higher yield and enantioselectivity. The substituents on the phosphine atom of dipyridyl ligand had an impact on the hydroalkynylation. Increase of sterics on the CTH-P-Phos (CTH-P-Xyl-Phos, **L8**) led to decreased yield. Among various solvents examined for ligand **L7**, the reaction conducted in 1,2-difluorobenzene provided slightly higher enantioselectivity. The absolute configuration of the product was determined by comparison of the optical rotation with authentic sample.

2.2 Substrate Scope. Having developed an effective catalyst system for the regio- and enantioselective hydroalkynylation, the scope of the substrates was further investigated. First, the reactivity of various β,γ-unsaturated amides synthesized from different amines was tested (Table 2). The length of alkyl chain on the nitrogen atom did not have a significant influence on the yield and enantioselectivity of hydroalkynylation (**3b**, **3c**). Furthermore, trisubstituted alkenyl amides with phenyl,

Table 2. **Scope of *N*-Substituted β,γ-Unsaturated Amides** [a]

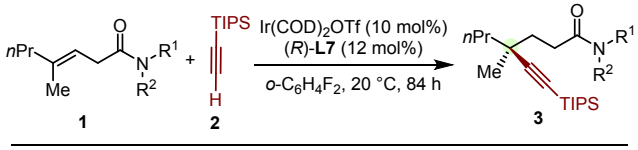

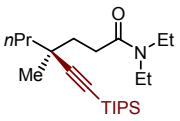

3a, 65%, 95:5 er

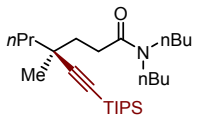

3b, 68%, 92.5:7.5 er

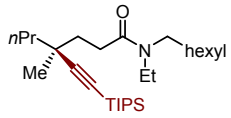

3c, 63%, 93:7 er

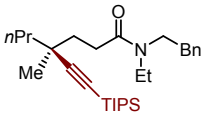

3d, 66%, 93:7 er

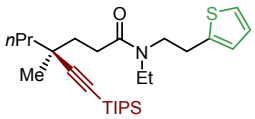

3e, 65%, 94:6 er

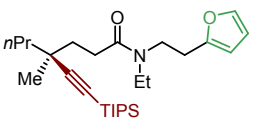

3f, 64%, 94.5:5.5 er

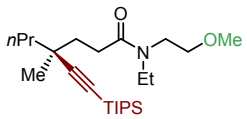

3g, 80%, 96.5:3.5 er

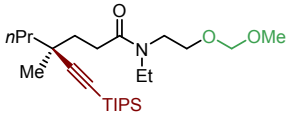

3h, 73%, 95.5:4.5 er

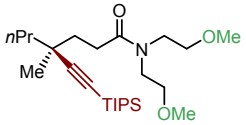

3i, 52%, 98.5:1.5 er

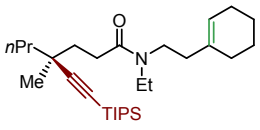

3j, 51%, 95.5:4.5 er

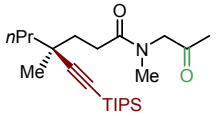

3k, <10%

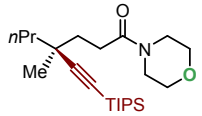

3l, 22%, 93:7 er

[a] See SI for details. Isolated yields were reported. The er values were determined by HPLC on a chiral stationary phase.

thienyl and furyl groups underwent hydroalkynylation smoothly, furnishing the desired products in good yield and enantioselectivity (**3d-3f**). The hydroalkynylation of substrates bearing ether (**3g**) and acetal (**3h**) gave slightly higher yields and enantioselectivities, probably as a result of their weak coordination with the catalyst. Further increase of the enantioselectivity was obtained when the amide contained two ether substituents although the yield was slightly lower (**3i**). Chemoselective hydroalkynylation was observed for a substrate containing two alkenes (**3j**). However, a terminal olefin or a ketone on the substrate was not tolerated (**3k**). The reaction of a Weinreb amide analogue provided modest yield of hydroalkynylation product and good enantioselectivity (**3l**).

Variations in the substituents of alkenes were also evaluated (Table 3). The reaction occurred with alkyl-substituted alkenes of different lengths in good yields and enantioselectivities (**3g**, **3j-3k**). The catalyst is sensitive to the sterics of the alkene. For example, when an isopentyl substituted alkene was used as a substrate, high yield of hydroalkynylation product was observed (**3l**). However, with an isobutyl-substituted alkene as the substrate, higher enantioselectivity but lower yield were observed (**3m**). No desired product was observed with further increase of the sterics on the alkene (**3n**). Moreover, functional groups including halide, ester, and ether were all tolerated (**3o-3s**). The distance between the alkene and the aryl group did not play a major role in the reaction (**3r**, **3s**). Thus, possible coordination of the substituent on the alkene to the metal center was not observed. Hydroalkynylation of an ethyl substituted alkene substrate afforded the product in low yield and decreased enantioselectivity, as a result of the increased steric hindrance and the difficulty to differentiate two similar alkyl groups (**3w**). Further effort is directed to solve this challenge.

Table 3. **Scope of Substituted Alkenyl Amides** [a]

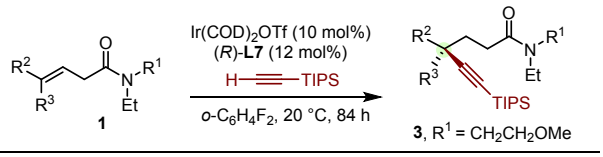

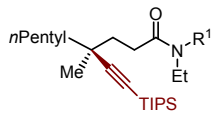

3m, 76%, 97:3 er

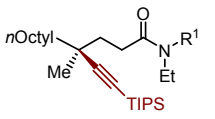

3n, 75%, 96:4 er

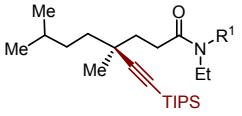

3o, 72%, 96:4 er

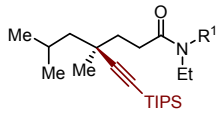

3p, 49%, 98.5:1.5 er

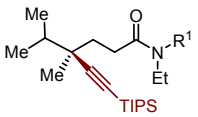

3q, <10%

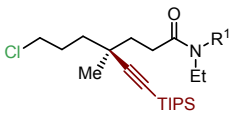

3r, 67%, 95.5:4.5 er

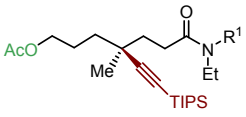

3s, 73%, 95:5 er

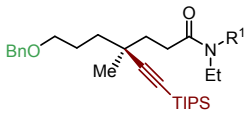

3t, 72%, 96.5:3.5 er

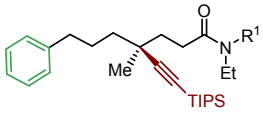

3u, 83%, 94:6 er

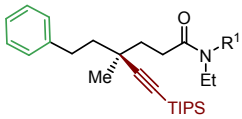

3v, 80%, 95:5 er

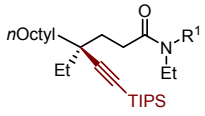

3w, 23%, 67:33 er

[a] See SI for details. Isolated yields were reported. The er values were determined by HPLC on a chiral stationary phase.

2.3 Transformation of Products. The silyl group in the hydroalkynylation product could be easily removed by TBAF, and the resulting terminal alkyne can be further manipulated to access various useful functionalities (Scheme 2). For example, semi-hydrogenation and complete hydrogenation of the terminal alkyne group afforded alkenyl and alkyl substituted quaternary carbon stereocenters respectively (**5a**, **5b**). In addition, Pd-catalyzed Sonogashira coupling installed an aryl group onto **4**, providing an alternative route to obtain the product from the hydroalkynylation with phenyl acetylenes (**5c**). Furthermore, the heteroaryl substituted quaternary carbon stereocenters were formed in high yields through a copper catalyzed click reaction (**5d**) and a Larock indole cyclization (**5e**). Lastly, **4** was readily converted to an acid substituted quaternary carbon stereocenters through Ru-catalyzed oxidation. High enantioselectivities were maintained in the products during these transformations. In addition to the alkyne, chemoselective transformation of the amide was

possible. Reduction of the amide afforded an amine with distal quaternary stereocenter (**5g**).

Scheme 2. Transformation of Alkynylation Products

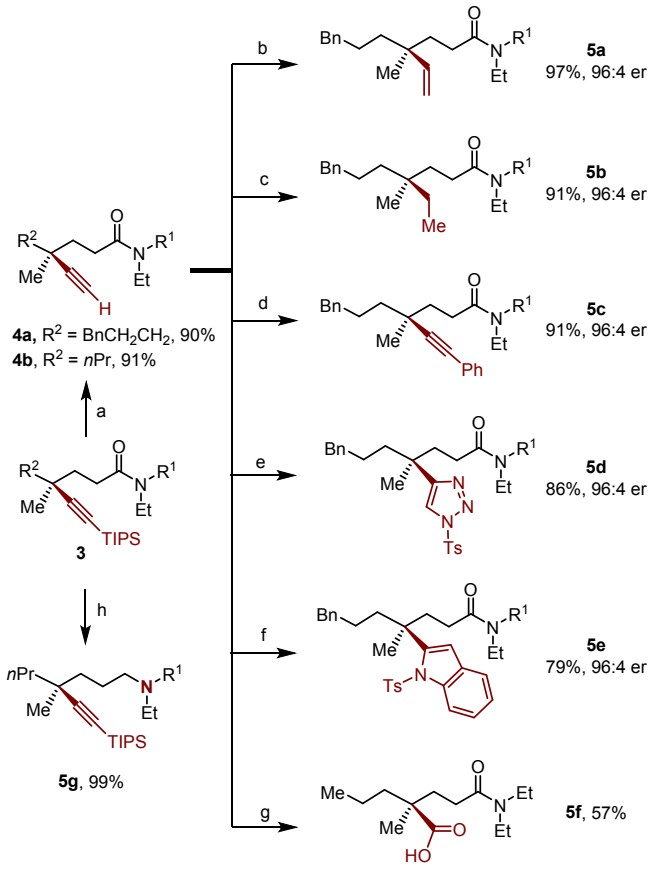

Reaction conditions: (a) TBAF, THF, RT. (b) H_2, Lindlar's catalyst, EtOAc, RT. (c) H_2, Pd/C, MeOH, RT. (d) PhI, $PdCl_2(PPh_3)_2$, CuI, NEt_3, THF, 45 °C. (e) TsN_3, CuTc, toluene, RT. (f) N-tosyl-2-iodobenzene, $Pd(PPh_3)_2Cl_2$, CuI, TMG, DMF, 40 °C. (g) $RuCl_3$, $NaIO_4$, CCl_4, MeCN, H_2O, RT. (h) $LiAlH_4$, THF. R^1 = CH_2CH_2OMe. Enantiomeric ratios of **5f** and **5g** were not determined.

2.4 Identification of the Catalyst Resting State. Monitoring the Ir catalyzed hydroalkynylation between **1u** and triisopropylsilylacetylene **2** revealed one major iridium complex throughout the course of the reaction. A singlet at 12.04 ppm was observed in the ^{31}P NMR spectrum, indicating that the two phosphorous atoms are equivalent. An Ir complex **6** was prepared from a combination of iridium precursor and the phosphine ligand. The spectral data of this compound were identical to the complex observed during the catalytic reaction (Equation 1). Thus, Ir complex **6** is the catalyst resting state of the catalytic reaction. These results provide basis for the following computational studies.

The hydroalkynylation of **1a** catalyzed by Ir complex **6** has similar kinetic profile to that of catalyzed by the *in-situ* generated catalyst, suggesting that complex **6** is a kinetically competent catalytic species.

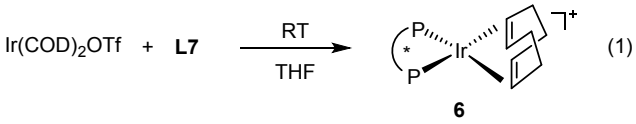

2.5 Measurement of Kinetic Isotope Effect (KIE). To determine the rate-limiting step of the catalytic hydroalkynylation, experiments to measure the kinetic isotope effect were conducted. To obtain reasonable rate for kinetic measurement, the reactions were conducted at 50 ℃ in dichlorobenzene. A comparison of the initial rates for the catalytic hydroalkynylations of **2a** and **2a-d** in separate vessels revealed a KIE of 1.3 (Scheme 3). This relatively small KIE suggested that the cleavage of the alkynyl C-H bond is less likely to be turnover-limiting.

Scheme 3. Kinetic Isotopic Effect of Alkyne

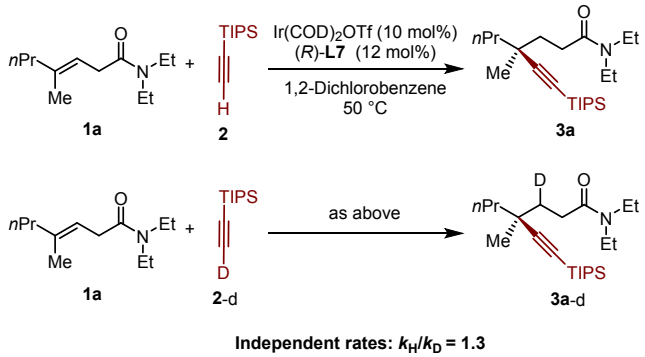

Independent rates: k_H/k_D = 1.3

To see whether the migratory insertion of the alkene is involved in the turnover-limiting step, the KIE of deuterated alkene was measured. If migratory insertion of the alkene is turnover-limiting, an inverse KIE would be observed (Scheme 4). The measurement of the reaction of **1u** and **1u**-d revealed a KIE of 0.90. This inverse KIE suggests that the migratory insertion of the alkene is likely involved in the turnover-limiting step.

Scheme 4. Kinetic Isotopic Effect of Alkene

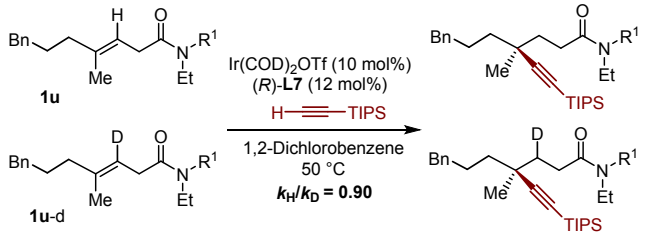

2.6 Origin of enantioselectivity. To gain insight into the origin of enantioselectivity, computational studies by density functional theory were conducted (Figure 1). The catalytic hydroalkynylation begins with the ligand exchange to generate an amide and alkyne bound Ir complex (**Int-7**). Oxidative addition of the terminal alkyne to the iridium center affords an alkynyl iridium hydride (**Int-8**), which undergoes migratory insertion of the alkene into the Ir−C bond to give a five membered iridacycle (**Int-10**). Finally, C-H reductive elimination delivers the hydroalkynylation product after dissociation.[19]

We computed the reaction pathways that lead to both enantiomers of the product. In both pathways, migratory insertions of the alkene have the highest activation free energies. The pathway leading to (*R*)-enantiomer has an activation barrier of 35.4 kcal/mol (**TS-2b**) while the pathway leading to (*S*)-enantiomer has an activation barrier of 30.2 kcal/mol (**TS-2a**). At least two factors contribute to the energy difference of **TS-2a** and **TS-2b** (Figure 2). First, the iridium hydride experiences significant repulsion with the ethyl group

of the substrate in **TS-2b** while such repulsion was not observed in **TS-2a** (2.27 vs 2.58 Å). Second, attractive C-H···O interactions of the carbonyl group with two aryl C-H bonds on the ligand were observed in **TS-2a** while only one weaker C-H···O interaction was found in **TS-2b** (2.25 and 2.26 vs 2.30 Å). The computation results indicate that the formation of (*S*)-enantiomer is favored over the formation of (*R*)-enantiomer by 5.2 kcal/mol, and an er of greater than 99.5:0.5 would be observed.

Experimentally, the absolute configuration was determined to be (*S*). This result is in agreement with the computation. In addition, the small KIE of deuterated alkyne and inverse KIE of deuterated alkene all agree with the computation that migratory insertion rather than C-H cleavage is rate limiting. However, the er obtained in the reaction of **1a** is only 95:5, significantly lower than the computed value. Therefore, we suspect that the enantioselectivity is not solely determined by the facial selectivity during migratory insertion (**TS-2a** vs **TS-2b**) but also by alternative processes.

In view of the Ir-H species involved in the reaction pathway, alkene isomerization could occur and have an impact on the enantioselectivity. If isomerization of the substrate from *E* to *Z* occurred, further hydroalkynylation of the *Z*-alkene would lead to the opposite enantiomer. Consequently, erosion of enantioselectivity would be observed. To test this hypothesis, both hydroalkynylation pathways from *Z*-alkene leading to the two enantiomers were also calculated (Figure 3). Similarly, the migratory insertions have the highest activation free energies for both pathways. The transition state **TS-2c,** connected to the (*R*)-enantiomer, has an activation barrier of 30.6 kcal/mol, while **TS-2d** which connects to the (*S*)-enantiomer, has an activation barrier of 35.6 kcal/mol. The activation free energies of the transition state structures from **TS-2a** to **TS-2d** indicate that **TS-2a** and **TS-2c** are the two major competing transition states leading to the major and minor enantiomers. In addition to the energy difference between **TS-2a** and **TS-2c**, the concentration difference of substrates **1**-*E* and **1**-*Z* also contribute to the relative rates of the pathways leading to the major and minor enantiomers. Therefore, the *E*/*Z* ratio of the alkene under the reaction conditions needs to be determined to provide proof for the alkene isomerization scenario.

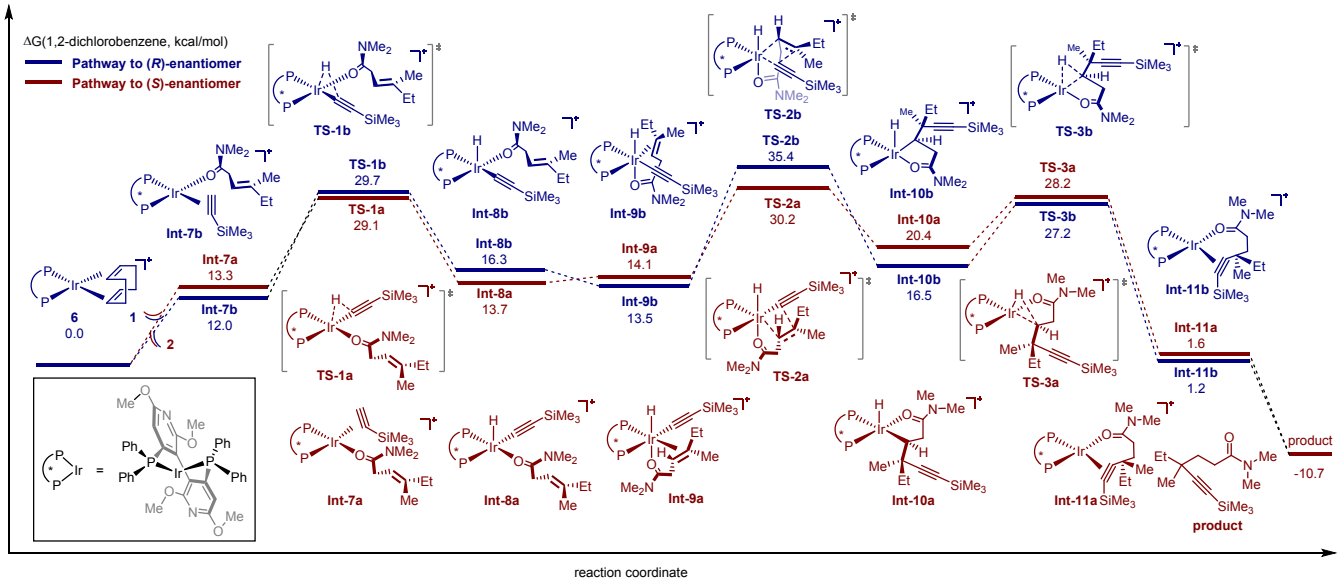

Figure 1. Computed pathways for catalytic hydroalkynylation. Calculations were carried out at the M06/6-311++g(d,p)/SDD//B3LYP/6-31g(d,p)/Lanl2dz level of theory.

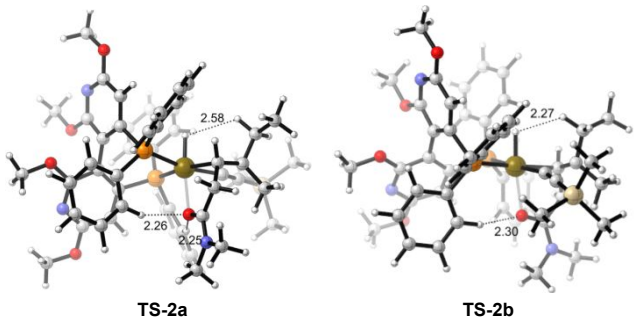

Figure 2. Transition state structures.

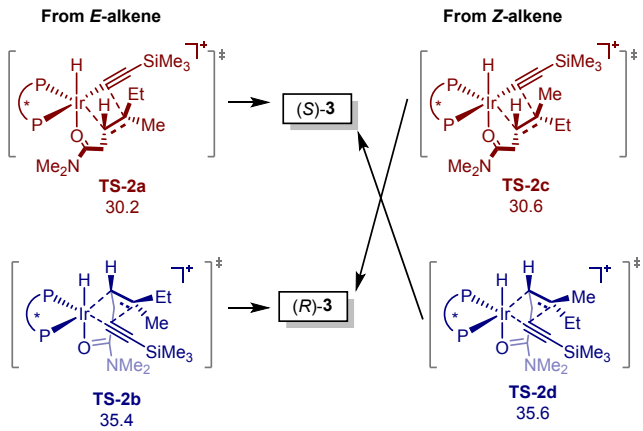

Figure 3. Computed transition states for migratory insertions.

To analyze the alkene isomerization process, control experiments were conducted (Scheme 5, A). We monitored the catalytic hydroalkynylation of **1u-*E***. Indeed, alkene isomerization was observed, although the concentration of the **1u-*Z*** was low because of the unfavorable thermodynamics. As the reaction proceeds, the *E*/*Z* ratio decreases slightly, while the enantiomeric ratio also decreases. The *E*/*Z* ratio of the alkene correlates roughly with the observed enantiomeric ratio.

To provide a better measurement of the alkene isomerization process, catalytic hydroalkynylation of the thermodynamically less favored **1u-*Z*** was conducted (Scheme 5, B). Indeed, significant amount of alkene isomerization was observed. As the reaction progresses, the *Z*/*E* ratio of remaining alkene decreases, while the er of product decreases as well. At higher temperature, the sense of enantioselectivity was even reversed due to significant alkene isomerization. Taken together, these results support that the enantioselectivity is not only determined by the enantio-face discrimination of the alkene, but also by an alkene isomerization process.

Scheme 5. Control Experiments

A. Hydroalkynylation of *E*-alkene

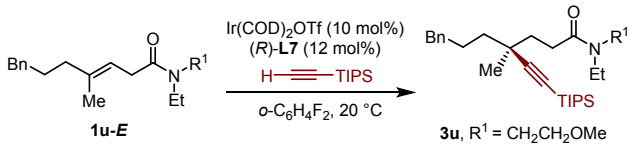

Entry	GC Yield	*E*/*Z* (**1u**)	er (**3u**)
1	8%	37 : 1	24 : 1
2	30%	13 : 1	17 : 1

B. Hydroalkynylation of *Z*-alkene

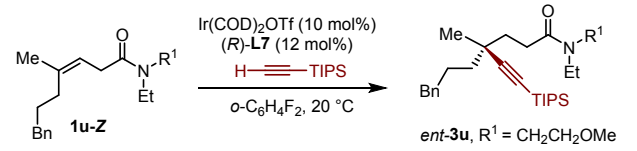

Entry	GC Yield	*Z*/*E* (**1u**)	er (*ent*-**3u**)
1	10%	16 : 1	5.7 : 1
2	20%	11 : 1	5.1 : 1
3	36%	4.1 : 1	4.6 : 1
4 (65 °C)	64%	1.2 : 1	1 : 1.1

2.7 Importance of the coordinating group. To probe the effect of the coordinating group on the reactivity and selectivity of Ir-catalyzed hydroalkynylation, transition states for the migratory insertion without amide coordination were computed (Figure 4). For both *E* and *Z*-alkenyl amides, four possible spatial arrangements of the alkenyl amide and the alkyne around the iridium center were considered. All these transition state structures have significantly higher activation free energies than that of the transition states with amide coordination (from **TS-2a** to **TS-2d**). Thus, the amide group played a major role to lower the activation barrier for the migratory insertion through coordination with the metal center.

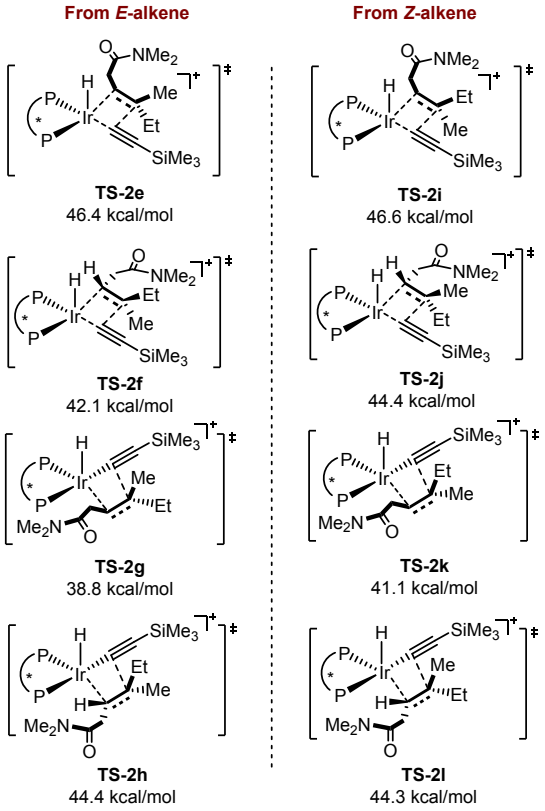

Figure 4. Computed transition states for migratory insertions without amide coordination.

To verify this effect, we tested the catalytic hydroalkynylation of a β,γ-unsaturated ester, in which the ester group is less coordinating than an amide. Indeed, no desired product was obtained, which provided support for the importance of the amide group (Equation 2).

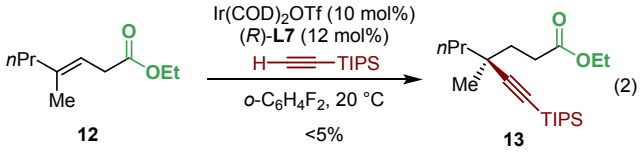

III. Conclusion

In summary, we have developed an iridium-catalyzed hydroalkynylation of trisubstituted β,γ-unsaturated amides. Complete γ-selectivity and high enantioselectivity were observed. This method provides an unprecedented strategy for the construction of alkyne-substituted acyclic quaternary carbon stereocenters. The alkyne group in these products undergoes a variety of transformations, thus allowing access to diverse chiral building blocks containing quaternary carbon stereocenters. The combined theoretical and experimental studies indicated that the enantioselectivity is not only determined by the facial selectivity of the alkene but also by an alkene isomerization process. Further computational studies revealed the importance of the amide group for the hydroalkynylation reaction. Improvement of the catalyst activity and application of this methodology in natural product synthesis are currently in progress in our laboratory.

ASSOCIATED CONTENT

Supporting Information.
Experimental procedures, characterization of new compounds and spectroscopic data are provided in the Supporting Information. This material is available free of charge via the Internet at http://pubs.acs.org.

AUTHOR INFORMATION

Corresponding Author

bijieli@mail.tsinghua.edu.cn

Notes

The authors declare no competing financial interests.

ACKNOWLEDGMENT

This work was supported by the National Natural Science Foundation of China (Grant No. 21672122 and No. 91856107), 111 Project (B16028) and National Program for Thousand Young Talents of China.

REFERENCES

(1) Newman, D. J.; Cragg, G. M. Natural Products as Sources of New Drugs from 1981 to 2014. *J. Nat. Prod.* **2016**, *79*, 629.

(2) (a) Bartholow, M. Top 200 drugs of 2011. *Pharm. Times* **10 July 2012**, *48–51*; (b) http://cbc.arizona.edu/njardarson/group/sites/default/files/Top200%20Pharmacetical%20Products%20by%20US%20Retail%20Sales%20in%202012_0.pdf.

(3) (a) Quasdorf, K. W.; Overman, L. E. Catalytic enantioselective synthesis of quaternary carbon stereocentres. *Nature* **2014**, *516*, 181; (b) Trost, B. M.; Jiang, C. Catalytic Enantioselective Construction of All-Carbon Quaternary Stereocenters. *Synthesis* **2006**, *2006*, 369; (c) Das, J. P.; Marek, I. Enantioselective synthesis of all-carbon quaternary stereogenic centers in acyclic systems. *Chem. Commun.* **2011**, *47*, 4593; (d) Feng, J.; Holmes, M.; Krische, M. J. Acyclic Quaternary Carbon Stereocenters via Enantioselective Transition Metal Catalysis. *Chem. Rev.* **2017**, *117*, 12564; (e) Christoffers, J.; Mann, A. Enantioselective Construction of Quaternary Stereocenters. *Angew. Chem. Int. Ed.* **2001**, *40*, 4591; (f) Ping, Y.; Li, Y.; Zhu, J.; Kong, W. Construction of Quaternary Stereocenters by Palladium-Catalyzed Carbopalladation-Initiated Cascade Reactions. *Angew. Chem. Int. Ed.* **2019**, *58*, 1562; (g) Liu, Y.; Han, S.-J.; Liu, W.-B.; Stoltz, B. M. Catalytic Enantioselective Construction of Quaternary Stereocenters: Assembly of Key Building Blocks for the Synthesis of Biologically Active Molecules. *Acc. Chem. Res.* **2015**, *48*, 740; (h) Zeng, X.-P.; Cao, Z.-Y.; Wang, Y.-H.; Zhou, F.; Zhou, J. Catalytic Enantioselective Desymmetrization Reactions to All-Carbon Quaternary Stereocenters. *Chem. Rev.* **2016**, *116*, 7330; (i) Wang, Z.; Yin, H.; Fu, G. C. Catalytic enantioconvergent coupling of secondary and tertiary electrophiles with olefins. *Nature* **2018**, *563*, 379; (j) Mei, T.-S.; Patel, H. H.; Sigman, M. S. Enantioselective construction of remote quaternary stereocentres. *Nature* **2014**, *508*, 340; (k) Bruffaerts, J.; Pierrot, D.; Marek, I. Efficient and stereodivergent synthesis of unsaturated acyclic fragments bearing contiguous stereogenic elements. *Nat. Chem.* **2018**, *10*, 1164.

(4) (a) Mourad, A. K.; Czekelius, C. Enantioselective Functionalization of Terminal Alkynes by Gold Catalysis. *Synlett* **2013**, *24*, 1459; (b) Zeng, M. S.; Herzon, S. B. Ruthenium-Catalyzed anti-Markovnikov Hydration and Reductive Hydration of Terminal Alkynes. *Aldrichimica Acta* **2014**, *47*, 55; (c) Trotuş, I.-T.; Zimmermann, T.; Schüth, F. Catalytic Reactions of Acetylene: A Feedstock for the Chemical Industry Revisited. *Chem. Rev.* **2014**, *114*, 1761; (d) Trost, B. M., Li, C.-J. *Modern Alkyne Chemistry: Catalytic and Atom-Economic Transformations*; Wiley: New York, 2014; (e) Schobert, H. Production of Acetylene and Acetylene-based Chemicals from Coal. *Chem. Rev.* **2014**, *114*, 1743; (f) Chinchilla, R.; Nájera, C. Chemicals from Alkynes with Palladium Catalysts. *Chem. Rev.* **2014**, *114*, 1783.

(5) Tsuchida, K.; Senda, Y.; Nakajima, K.; Nishibayashi, Y. Construction of Chiral Tri- and Tetra-Arylmethanes Bearing Quaternary Carbon Centers: Copper-Catalyzed Enantioselective Propargylation of Indoles with Propargylic Esters. *Angew. Chem. Int. Ed.* **2016**, *55*, 9728.

(6) Shemet, A.; Carreira, E. M. Total Synthesis of (−)-Rhazinilam and Formal Synthesis of (+)-Eburenine and (+)-Aspidospermidine: Asymmetric Cu-Catalyzed Propargylic Substitution. *Org. Lett.* **2017**, *19*, 5529.

(7) Zhang, Y.-C.; Zhang, B.-W.; Geng, R.-L.; Song, J. Enantioselective [3 + 2] Cycloaddition Reaction of Ethynylethylene Carbonates with Malononitrile Enabled by Organo/Metal Cooperative Catalysis. *Org. Lett.* **2018**, *20*, 7907.

(8) (a) Mourad, A. K.; Leutzow, J.; Czekelius, C. Anion-Induced Enantioselective Cyclization of Diynamides to Pyrrolidines Catalyzed by Cationic Gold Complexes. *Angew. Chem. Int. Ed.* **2012**, *51*, 11149; (b) Czekelius, C. Total Synthesis of Mesembrine – The Construction of Quaternary Stereocenters by Gold-Catalyzed Diyne Desymmetrization. *Isr. J. Chem.* **2018**, *58*, 568.

(9) Dabrowski, J. A.; Gao, F.; Hoveyda, A. H. Enantioselective Synthesis of Alkyne-Substituted Quaternary Carbon Stereogenic Centers through NHC−Cu-Catalyzed Allylic Substitution Reactions with (i-Bu)2(Alkynyl)aluminum Reagents. *J. Am. Chem. Soc.* **2011**, *133*, 4778.

(10) For non-catalytic methods: (a) Pérez, I.; Yuste, F.; Sánchez-Obregón, R.; Toscano, R. A.; Alemán, J.; Marzo, L.; Martín Castro, A. M.; Alonso, I.; García Ruano, J. L. Synthesis of Enantiopure 1,5-Enynes and 1,5-Diynes with Propargylic Quaternary Centers. *Eur. J. Org. Chem.* **2015**, *2015*, 3314; (b) Wang, Y.; Noble, A.; Myers, E. L.; Aggarwal, V. K. Enantiospecific Alkynylation of Alkylboronic Esters. *Angew. Chem. Int. Ed.* **2016**, *55*, 4270; (c) Bang, J.; Oh, C.; Lee, E.; Jeong, H.; Lee, J.; Ryu, J. Y.; Kim, J.; Yu, C.-M. A Regulation of Regiodivergent Routes for Enantioselective Aldol Addition of 2-Alkyl Allenoates with Aldehydes: α-Addition versus γ-Addition. *Org. Lett.* **2018**, *20*, 1521; For organocatalytic methods: (d) Wendlandt, A. E.; Vangal, P.; Jacobsen, E. N. Quaternary stereocentres via an enantioconvergent catalytic SN1 reaction. *Nature* **2018**, *556*, 447; (e) Chen, Z.-C.; Chen, P.; Chen, Z.; Ouyang, Q.; Liang, H.-P.; Du, W.; Chen, Y.-C. Organocatalytic Enantioselective 1,3-Difunctionalizations of Morita–Baylis–Hillman Carbonates. *Org. Lett.* **2018**, *20*, 6279; (f) Hashimoto, T.; Sakata, K.; Maruoka, K. α-Chiral Acetylenes Having an All-Carbon Quaternary Center: Phase Transfer Catalyzed Enantioselective α Alkylation of α-Alkyl-α-alkynyl Esters. *Angew. Chem. Int. Ed.* **2009**, *48*, 5014; (g) Poulsen, T. B.; Bernardi, L.; Alemán, J.; Overgaard, J.; Jørgensen, K. A. Organocatalytic Asymmetric Direct α-Alkynylation of Cyclic β-Ketoesters. *J. Am. Chem. Soc.* **2007**, *129*, 441; (h) Wang, D.; Zhang, L.; Luo, S. Enantioselective Decarboxylative α-Alkynylation of β-Ketocarbonyls via a Catalytic α-Imino Radical Intermediate. *Org. Lett.* **2017**, *19*, 4924; Related ketone α-alkynylation: (i) Roy, A.; Das, M. K.; Chaudhuri, S.; Bisai, A. Transition-Metal Free Oxidative Alkynylation of 2-Oxindoles with Ethynylbenziodoxolone (EBX) Reagents. *J. Org. Chem.* **2018**, *83*, 403; (j) Wang, Z.; Zhang, Z.; Yao, Q.; Liu, X.; Cai, Y.; Lin, L.; Feng, X. Highly Stereoselective Conjugate Addition and α-Alkynylation Reaction with Electron-Deficient Alkynes

Catalyzed by Chiral Scandium(III) Complexes. *Chem. Eur. J.* **2013**, *19*, 8591; For alkyne not directly attached to the chiral center: (k) Jonker, S. J. T.; Diner, C.; Schulz, G.; Iwamoto, H.; Eriksson, L.; Szabó, K. J. Catalytic asymmetric propargyl- and allylboration of hydrazonoesters: a metal-free approach to sterically encumbered chiral α-amino acid derivatives. *Chem. Commun.* **2018**, *54*, 12852; (l) Zhao, J.; Jonker, S. J. T.; Meyer, D. N.; Schulz, G.; Tran, C. D.; Eriksson, L.; Szabó, K. J. Copper-catalyzed synthesis of allenylboronic acids. Access to sterically encumbered homopropargylic alcohols and amines by propargylboration. *Chem. Sci.* **2018**, *9*, 3305; For two-substrates example: (m) Wiest, J. M.; Conner, M. L.; Brown, M. K. Allenoates in Enantioselective [2+2] Cycloadditions: From a Mechanistic Curiosity to a Stereospecific Transformation. *J. Am. Chem. Soc.* **2018**, *140*, 15943.

(11) (a) Coombs, J. R.; Morken, J. P. Catalytic Enantioselective Functionalization of Unactivated Terminal Alkenes. *Angew. Chem. Int. Ed.* **2016**, *55*, 2636; (b) Bower, J. F.; Kim, I. S.; Patman, R. L.; Krische, M. J. Catalytic Carbonyl Addition through Transfer Hydrogenation: A Departure from Preformed Organometallic Reagents. *Angew. Chem. Int. Ed.* **2009**, *48*, 34. Byproduct-free reactions that generate acyclic quaternary carbon stereocenters are highly uncommon: (c) Shi, W.-J.; Zhang, Q.; Xie, J.-H.; Zhu, S.-F.; Hou, G.-H.; Zhou, Q.-L. Highly Enantioselective Hydrovinylation of α-Alkyl Vinylarenes. An Approach to the Construction of All-Carbon Quaternary Stereocenters. *J. Am. Chem. Soc.* **2006**, *128*, 2780; (d) Zhang, A.; RajanBabu, T. V. All-Carbon Quaternary Centers via Catalytic Asymmetric Hydrovinylation. New Approaches to the Exocyclic Side Chain Stereochemistry Problem. *J. Am. Chem. Soc.* **2006**, *128*, 5620; (e) Feng, J.; Garza, V. J.; Krische, M. J. Redox-Triggered C–C Coupling of Alcohols and Vinyl Epoxides: Diastereo- and Enantioselective Formation of All-Carbon Quaternary Centers via tert-(Hydroxy)-Prenylation. *J. Am. Chem. Soc.* **2014**, *136*, 8911; (f) Nguyen, K. D.; Herkommer, D.; Krische, M. J. Enantioselective Formation of All-Carbon Quaternary Centers via C–H Functionalization of Methanol: Iridium-Catalyzed Diene Hydrohydroxymethylation. *J. Am. Chem. Soc.* **2016**, *138*, 14210; (g) Holmes, M.; Nguyen, K. D.; Schwartz, L. A.; Luong, T.; Krische, M. J. Enantioselective Formation of CF3-Bearing All-Carbon Quaternary Stereocenters via C–H Functionalization of Methanol: Iridium Catalyzed Allene Hydrohydroxymethylation. *J. Am. Chem. Soc.* **2017**, *139*, 8114.

(12) (a) Knöpfel, T. F.; Zarotti, P.; Ichikawa, T.; Carreira, E. M. Catalytic, Enantioselective, Conjugate Alkyne Addition. *J. Am. Chem. Soc.* **2005**, *127*, 9682; (b) Nishimura, T.; Katoh, T.; Takatsu, K.; Shintani, R.; Hayashi, T. Rhodium-Catalyzed Asymmetric Rearrangement of Alkynyl Alkenyl Carbinols: Synthetic Equivalent to Asymmetric Conjugate Alkynylation of Enones. *J. Am. Chem. Soc.* **2007**, *129*, 14158; (c) Nishimura, T.; Guo, X.-X.; Uchiyama, N.; Katoh, T.; Hayashi, T. Steric Tuning of Silylacetylenes and Chiral Phosphine Ligands for Rhodium-Catalyzed Asymmetric Conjugate Alkynylation of Enones. *J. Am. Chem. Soc.* **2008**, *130*, 1576; (d) Nishimura, T.; Tokuji, S.; Sawano, T.; Hayashi, T. Rhodium-Catalyzed Asymmetric Conjugate Alkynylation of Enones with Alkynylsilanols. *Org. Lett.* **2009**, *11*, 3222; (e) Nishimura, T.; Sawano, T.; Hayashi, T. Asymmetric Synthesis of β-Alkynyl Aldehydes by Rhodium-Catalyzed Conjugate Alkynylation. *Angew. Chem. Int. Ed.* **2009**, *48*, 8057; (f) Fillion, E.; Zorzitto, A. K. Enantioselective Rhodium-Catalyzed Conjugate Alkynylation of 5-Benzylidene Meldrum's Acids with TMS-acetylene. *J. Am. Chem. Soc.* **2009**, *131*, 14608; (g) Yazaki, R.; Kumagai, N.; Shibasaki, M. Direct Catalytic Asymmetric Conjugate Addition of Terminal Alkynes to α,β-Unsaturated Thioamides. *J. Am. Chem. Soc.* **2010**, *132*, 10275; (h) Yazaki, R.; Kumagai, N.; Shibasaki, M. Cooperative Activation of Alkyne and Thioamide Functionalities; Direct Catalytic Asymmetric Conjugate Addition of Terminal Alkynes to α,β-Unsaturated Thioamides. *Chem. Asian J.* **2011**, *6*, 1778; (i) Nishimura, T.; Sawano, T.; Ou, K.; Hayashi, T. Cobalt-catalyzed conjugate addition of silylacetylenes to α,β-unsaturated ketones. *Chem. Commun.* **2011**, *47*, 10142; (j) Sawano, T.; Ashouri, A.; Nishimura, T.; Hayashi, T. Cobalt-Catalyzed Asymmetric 1,6-Addition of (Triisopropylsilyl)-acetylene to α,β,γ,δ-Unsaturated Carbonyl Compounds. *J. Am. Chem. Soc.* **2012**, *134*, 18936; (k) Sanz-Marco, A.; Garcia-Ortiz, A.; Blay, G.; Pedro, J. R. Catalytic asymmetric conjugate addition of terminal alkynes to [small beta]-trifluoromethyl [small alpha],[small beta]-enones. *Chem. Commun.* **2014**, *50*, 2275; (l) Dou, X.; Huang, Y.; Hayashi, T. Asymmetric Conjugate Alkynylation of Cyclic α,β-Unsaturated Carbonyl Compounds with a Chiral Diene Rhodium Catalyst. *Angew. Chem. Int. Ed.* **2016**, *55*, 1133; (m) Zhi, Y.; Huang, J.; Liu, N.; Lu, T.; Dou, X. Rhodium-Catalyzed Asymmetric Conjugate Alkynylation of β,γ-Unsaturated α-Ketoesters. *Org. Lett.* **2017**, *19*, 2378; (n) Choo, K.-L.; Lautens, M. Rhodium-Catalyzed Asymmetric Conjugate Alkynylation/Aldol Cyclization Cascade for the Formation of α-Propargyl-β-hydroxyketones. *Org. Lett.* **2018**, *20*, 1380; (o) Sanz-Marco, A.; Blay, G.; Vila, C.; Pedro, J. R. Catalytic Enantioselective Conjugate Alkynylation of β-Aryl-β-trifluoromethyl Enones Constructing Propargylic All-Carbon Quaternary Stereogenic Centers. *Org. Lett.* **2016**, *18*, 3538.

(13) (a) Fan, B.-M.; Yang, Q.-j.; Hu, J.; Fan, C.-l.; Li, S.-f.; Yu, L.; Huang, C.; Tsang, W. W.; Kwong, F. Y. Asymmetric Hydroalkynylation of Norbornadienes Promoted by Chiral Iridium Catalysts. *Angew. Chem. Int. Ed.* **2012**, *51*, 7821; (b) Sawano, T.; Ou, K.; Nishimura, T.; Hayashi, T. Cobalt-catalyzed asymmetric addition of silylacetylenes to oxa- and azabenzonorbornadienes. *Chem. Commun.* **2012**, *48*, 6106; (c) Sawano, T.; Ou, K.; Nishimura, T.; Hayashi, T. Cobalt-Catalyzed Asymmetric Addition of Silylacetylenes to 1,1-Disubstituted Allenes. *J. Org. Chem.* **2013**, *78*, 8986; (d) Hu, J.; Yang, Q.; Xu, J.; Huang, C.; Fan, B.; Wang, J.; Lin, C.; Bian, Z.; Chan, A. S. C. Iridium-catalyzed asymmetric hydroalkynylation reactions of oxabenzonorbornadienes. *Org. Biomol. Chem.* **2013**, *11*, 814; (e) Fan, B.; Xu, J.; Yang, Q.; Li, S.; Chen, H.; Liu, S.; Yu, L.; Zhou, Y.; Wang, L. Rh-Catalyzed Highly Enantioselective Hydroalkynylation Reaction of Norbornadiene Derivatives. *Org. Lett.* **2013**, *15*, 5956; (f) Yang, Q.; Choy, P. Y.; Fan, B.; Kwong, F. Y. Enantioselective Hydroalkynylation of Non-Polar Carbon-Carbon Double Bonds: Iridium-Catalyzed Asymmetric Addition Reaction of Terminal Alkyne C-H Bonds to Substituted Norbornadienes. *Adv. Synth. Catal.* **2015**, *357*, 2345.

(14) (a) Wang, Z.-X.; Bai, X.-Y.; Li, B.-J. Recent Progress of Transition-Metal-Catalyzed Enantioselective Hydroalkynylation of Alkenes. *Synlett* **2017**, *28*, 509; For alternative approaches: (b) Chen, Z. M.; Nervig, C. S.; DeLuca, R. J.; Sigman, M. S. Palladium-Catalyzed Enantioselective Redox-Relay Heck Alkynylation of Alkenols To Access Propargylic Stereocenters. *Angew. Chem. Int. Ed.* **2017**, *56*, 6651; (c) Fu, L.; Zhou, S.; Wan, X.; Chen, P.; Liu, G. Enantioselective Trifluoromethylalkynylation of Alkenes via Copper-Catalyzed Radical Relay. *J. Am. Chem. Soc.* **2018**, *140*, 10965; (d) Cui, X. Y.; Ge, Y.; Tan, S. M.; Jiang, H.; Tan, D.; Lu, Y.; Lee, R.; Tan, C. H. (Guanidine)copper Complex-Catalyzed Enantioselective Dynamic Kinetic Allylic Alkynylation under Biphasic Condition. *J. Am. Chem. Soc.* **2018**, *140*, 8448; (e) Yeqiang, H.; Ding, Y.; Zhou, T.; Yan, S.-Y.; Song, H.; Shi, B.-F. Pd(II)-Catalyzed Enantioselective Alkynylation of Unbiased Methylene C(sp3)–H Bonds Using 3,3'-Fluorinated-BINOL as Chiral Ligand. *J. Am. Chem. Soc.* **2019**, *141*, 4558.

(15) For our work on amide assisted asymmetric functionalization of alkenes: (a) Bai, X.-Y.; Wang, Z.-X.; Li, B.-J. Iridium-Catalyzed Enantioselective Hydroalkynylation of

Enamides for the Synthesis of Homopropargyl Amides. *Angew. Chem. Int. Ed.* **2016**, *55*, 9007; (b) Wang, Z.-X.; Bai, X.-Y.; Yao, H.-C.; Li, B.-J. Synthesis of Amides with Remote Stereocenters by Catalytic Asymmetric γ-Alkynylation of α,β-Unsaturated Amides. *J. Am. Chem. Soc.* **2016**, *138*, 14872; (c) Bai, X.-Y.; Zhang, W.-W.; Li, Q.; Li, B.-J. Highly Enantioselective Synthesis of Propargyl Amides through Rh-Catalyzed Asymmetric Hydroalkynylation of Enamides: Scope, Mechanism, and Origin of Selectivity. *J. Am. Chem. Soc.* **2018**, *140*, 506; (d) Gao, T.-t.; Zhang, W.-W.; Sun, X.; Lu, H.-X.; Li, B.-J. Stereodivergent Synthesis through Catalytic Asymmetric Reversed Hydroboration. *J. Am. Chem. Soc.* **2019**, *141*, 4670.

(16) (a) Wang, H.; Bai, Z.; Jiao, T.; Deng, Z.; Tong, H.; He, G.; Peng, Q.; Chen, G. Palladium-Catalyzed Amide-Directed Enantioselective Hydrocarbo-functionalization of Unactivated Alkenes Using a Chiral Monodentate Oxazoline Ligand. *J. Am. Chem. Soc.* **2018**, *140*, 3542; (b) Nimmagadda, S. K.; Liu, M.; Karunananda, M. K.; Gao, D. W.; Apolinar, O.; Chen, J. S.; Liu, P.; Engle, K. M. Catalytic, Enantioselective alpha-Alkylation of Azlactones with Nonconjugated Alkenes by Directed Nucleopalladation. *Angew. Chem. Int. Ed.* **2019**, *58*, 3923; (c) Liu, Z.; Li, X.; Zeng, T.; Engle, K. M. Directed, Palladium(II)-Catalyzed Enantioselective anti-Carboboration of Alkenyl Carbonyl Compounds. *ACS Catalysis* **2019**, 3260; (d) Smith, S. M.; Thacker, N. C.; Takacs, J. M. Efficient amide-directed catalytic asymmetric hydroboration. *J. Am. Chem. Soc.* **2008**, *130*, 3734; (e) Smith, S. M.; Takacs, J. M. Amide-Directed Catalytic Asymmetric Hydroboration of Trisubstituted Alkenes. *J. Am. Chem. Soc.* **2010**, *132*, 1740; (f) Derosa, J.; Kleinmans, R.; Tran, V. T.; Karunananda, M. K.; Wisniewski, S. R.; Eastgate, M. D.; Engle, K. M. Nickel-Catalyzed 1,2-Diarylation of Simple Alkenyl Amides. *J. Am. Chem. Soc.* **2018**, *140*, 17878; (g) Zultanski, S. L.; Fu, G. C. Catalytic Asymmetric γ-Alkylation of Carbonyl Compounds via Stereoconvergent Suzuki Cross-Couplings. *J. Am. Chem. Soc.* **2011**, *133*, 15362; (h) Basnet, P.; Dhungana, R. K.; Thapa, S.; Shrestha, B.; Kc, S.; Sears, J. M.; Giri, R. Ni-Catalyzed Regioselective β,δ-Diarylation of Unactivated Olefins in Ketimines via Ligand-Enabled Contraction of Transient Nickellacycles: Rapid Access to Remotely Diarylated Ketones. *J. Am. Chem. Soc.* **2018**, *140*, 7782; (i) Shibata, T.; Tsuchikama, K.; Pan, S. Cationic Iridium-Catalyzed Synthesis Initiated by the Cleavage of C-H, N-H, and C-O Bonds. *J. Synth. Org. Chem. Jpn.* **2013**, *71*, 1182; (j) Vanable, E. P.; Kennemur, J. L.; Joyce, L. A.; Ruck, R. T.; Schultz, D. M.; Hull, K. L. Rhodium-Catalyzed Asymmetric Hydroamination of Allyl Amines. *J. Am. Chem. Soc.* **2019**, *141*, 739.

(17) (a) Werner, E. W.; Mei, T.-S.; Burckle, A. J.; Sigman, M. S. Enantioselective Heck Arylations of Acyclic Alkenyl Alcohols Using a Redox-Relay Strategy. *Science* **2012**, *338*, 1455; (b) Vasseur, A.; Bruffaerts, J.; Marek, I. Remote functionalization through alkene isomerization. *Nat. Chem.* **2016**, *8*, 209; (c) Patel, H. H.; Sigman, M. S. Enantioselective Palladium-Catalyzed Alkenylation of Trisubstituted Alkenols To Form Allylic Quaternary Centers. *J. Am. Chem. Soc.* **2016**, *138*, 14226.

(18) Xie, J.-H.; Zhou, Q.-L. Chiral Diphosphine and Monodentate Phosphorus Ligands on a Spiro Scaffold for Transition-Metal-Catalyzed Asymmetric Reactions. *Acc. Chem. Res.* **2008**, *41*, 581.

(19) (a) Sevov, C. S.; Hartwig, J. F. Iridium-Catalyzed Oxidative Olefination of Furans with Unactivated Alkenes. *J. Am. Chem. Soc.* **2014**, *136*, 10625; (b) Sevov, C. S.; Hartwig, J. F. Iridium-Catalyzed Intermolecular Asymmetric Hydroheteroarylation of Bicycloalkenes. *J. Am. Chem. Soc.* **2013**, *135*, 2116; (c) Hatano, M.; Ebe, Y.; Nishimura, T.; Yorimitsu, H. Asymmetric Alkylation of N-Sulfonylbenzamides with Vinyl Ethers via C–H Bond Activation Catalyzed by Hydroxoiridium/Chiral Diene Complexes. *J. Am. Chem. Soc.* **2016**, *138*, 4010.

Insert Table of Contents artwork here